1 **Hnf4a mediates microbial control of intestinal gene expression and inflammation**

2 James M. Davison[1,2], Colin R. Lickwar[1], Lingyun Song[3], Ghislain Breton[4], Gregory E. Crawford[3]

3 and John F. Rawls[1,‡]

4 [1]Department of Molecular Genetics and Microbiology, Center for the Genomics of Microbial

5 Systems, Duke University, Durham, North Carolina 27710, USA; [2]Department of Cell Biology and

6 Physiology, University of North Carolina, Chapel Hill, North Carolina 27599, USA; [3]Department of

7 Pediatrics, Division of Medical Genetics, Center for Genomic and Computational Biology, Duke

8 University, Durham, North Carolina 27708, USA; [4]Department of Integrative Biology and

9 Pharmacology, McGovern Medical School, Houston, Texas 77030, USA; [‡]Corresponding Author.

10 **ABSTRACT**

11 Microbiota influence diverse aspects of intestinal epithelial physiology and disease in part by

12 controlling tissue-specific transcription of host genes. However, host genomic mechanisms

13 mediating microbial control of host gene expression are poorly understood. Using an unbiased

14 screening strategy, we found that the zebrafish Hepatic nuclear factor 4 alpha (Hnf4a)

15 transcription factor specifically binds and activates a microbiota-suppressed intestinal epithelial

16 transcriptional enhancer. Genetic analysis disclosed that zebrafish *hnf4a* activates nearly half of

17 the genes that are suppressed by microbiota, suggesting microbiota negatively regulate Hnf4a.

18 In support, analysis of genomic architecture in mouse intestinal epithelial cells revealed that

19 microbiota colonization leads to activation or inactivation of hundreds of enhancers along with

20 drastic genome-wide reduction of Hnf4a and Hnf4g occupancy. Interspecies meta-analysis

21 suggests Hnf4a may mediate microbial contributions to inflammatory bowel disease

22 pathogenesis. These results indicate Hnf4a plays a critical conserved role in maintaining

23 intestinal homeostasis in response to microbiota and inflammation.

24

28   **INTRODUCTION**

29   All animals face the fundamental challenge of building and maintaining diverse tissues while

30   remaining sensitive and responsive to their environment. This is most salient in the intestinal

31   epithelium which performs important roles in nutrient absorption and barrier function while being

32   constantly exposed to complex microbial communities (microbiota) and nutrients within the

33   intestinal lumen. The presence and composition of microbiota in the intestinal lumen influence

34   diverse aspects of intestinal development and physiology including dietary nutrient metabolism

35   and absorption, intestinal epithelial renewal, and edification of the host immune system.

36   Abnormal host-microbiota interactions are strongly implicated in the pathogenesis of

37   inflammatory bowel diseases (IBD), including Crohn's disease (CD) and ulcerative colitis (UC)

38   (Sartor and Wu 2016). Studies in mouse and zebrafish models of IBD have established that

39   impaired intestinal epithelial cell (IEC) responses to microbiota are a key aspect of disease

40   progression (Bates et al. 2007; Kamada et al. 2013; Marjoram et al. 2015). Improved

41   understanding of the molecular mechanisms by which microbiota evoke host responses in the

42   intestinal epithelium can be expected to lead to new strategies for preventing or treating IBD

43   and other microbiota-associated diseases.

44   The ability of IEC to maintain their physiologic functions and respond appropriately to microbial

45   stimuli is facilitated through regulation of gene transcription. Genome-wide comparison of

46   transcript levels in intestinal tissue or isolated IEC from mice reared in the absence of microbes

47   (germ-free or GF) to those colonized with a microbiota (conventionalized or CV) have revealed

48   hundreds of genes that have significantly increased or decreased mRNA levels following

49   microbiota colonization (Camp et al. 2014). Interestingly, many mouse genes that are

50   transcriptionally regulated by microbiota have zebrafish homologs that are similarly responsive,

51   suggesting the existence of evolutionarily-conserved regulatory mechanisms (Rawls et al.

52   2004). For example, the protein hormone Angiopoetin-like 4 (Angptl4, also called Fiaf) is

3

53   encoded by a single ortholog in the mouse and zebrafish genomes, and microbiota colonization

54   results in significant reductions in transcript levels in the small intestinal epithelium of both host

55   species (Bäckhed et al. 2004; Camp et al. 2012). Whereas these impacts of microbiota on host

56   IEC transcriptomes and their downstream consequences have been extensively documented,

57   the upstream transcriptional regulatory mechanisms remain poorly understood.

58   Specification and tuning of gene transcription proceeds in part through interactions between

59   transcription factors (TFs) and their sequence-specific binding to *cis*-regulatory DNA. *Cis*-

60   regulatory regions (CRRs) harbor binding sites for multiple activating or repressing TFs and are

61   generally associated with nucleosome depletion and specific post-translational modifications of

62   histone proteins within adjacent nucleosomes when acting as poised (H3K4me1) or active

63   (H3K27ac) enhancers (Creyghton et al. 2010). Antibiotic administration can impact transcript

64   levels and histone modifications in IECs (Thaiss et al. 2016), however it's unclear if these

65   changes are indirect effects caused by alterations to microbiota composition, direct effects of

66   the antibiotic on host cells, or by the effects of remaining antibiotic-resistant microbiota (Morgun

67   et al. 2015). Previous studies have shown that histone deacetylase 3 is required in IECs to

68   maintain intestinal homeostasis in the presence of microbiota (Alenghat et al. 2013), and that

69   overall histone acetylation and methylation in the intestine is altered by microbiota colonization

70   (Krautkramer et al. 2016). However, the direct and specific effects of the microbiota on host

71   CRRs and subsequent transcriptional responses in IECs remain unknown.

72   Our previous work predicted key roles for one or more nuclear receptor TFs in microbial down

73   regulation of IEC gene expression (Camp et al. 2014), but the specific TF(s) were not identified.

74   Nuclear receptors are ideal candidate TFs for integrating microbe-derived signals, since for

75   many their transcriptional activity can be positively or negatively regulated by the binding of

76   metabolic or hormonal ligands (Evans and Mangelsdorf 2014). However, the roles of nuclear

77   receptors in host responses remain poorly understood, and no previous study has defined the

78   impact of microbiota on nuclear receptor DNA binding. Nuclear receptors are a metazoan

79   innovation. The earliest animals encoded a single nuclear receptor orthologous to Hepatocyte

80   nuclear factor 4 (Hnf4; nuclear receptor subfamily NR2A) (Bridgham et al. 2010). Despite

81   subsequent duplication and diversification, distinct Hnf4 TFs remain encoded in extant animals

82   including mammals (Hnf4a, Hnf4g) and fishes (Hnf4a, Hnf4b, Hnf4g) (Supplemental Fig. S1G).

83   Hnf4a serves particularly important roles in IECs, where it binds CRRs and activates expression

84   of genes involved in IEC maturation and function (Stegmann et al. 2006). IEC-specific knockout

85   of mouse *Hnf4a* results in spontaneous intestinal inflammation similar to human IBD (Darsigny

86   et al. 2009). In accord, genetic variants at human *HNF4A* are associated with IBD as well as

87   colon cancer (Marcil et al. 2012; Chellappa et al. 2016). Hnf4a is predicted to bind a majority of

88   IBD-linked CRRs and regulate IBD-linked genes (Haberman et al. 2014; Meddens et al. 2016).

89   Similarly, genetic variants near human *HNF4G* have been associated with obesity and IBD

90   (Franke et al. 2007; Berndt et al. 2013). Importantly, these diverse roles for Hnf4 TFs in host

91   physiology have only been studied in host animals colonized with microbiota. Therefore, the role

92   of Hnf4 in host-microbiota interactions and the implications for human IBD remain unknown.

93   **RESULTS**

94   ***hnf4a* is essential for transcriptional activity from a microbiota-suppressed cis-regulatory**

95   **DNA region**

96   To identify transcriptional regulatory mechanisms underlying microbial control of host gene

97   expression, we took advantage of a previously identified microbiota-responsive CRR termed

98   in3.4 located within the third intron of zebrafish *angptl4* (Fig. 1A). A GFP reporter construct

99   under control of in3.4 termed *in3.4:cfos:gfp* drives tissue specific expression of GFP in zebrafish

100   IEC and is suppressed by microbiota colonization, recapitulating the microbial suppression of

101   zebrafish *angptl4* (Camp et al. 2012). However, the factor(s) that mediate microbial suppression
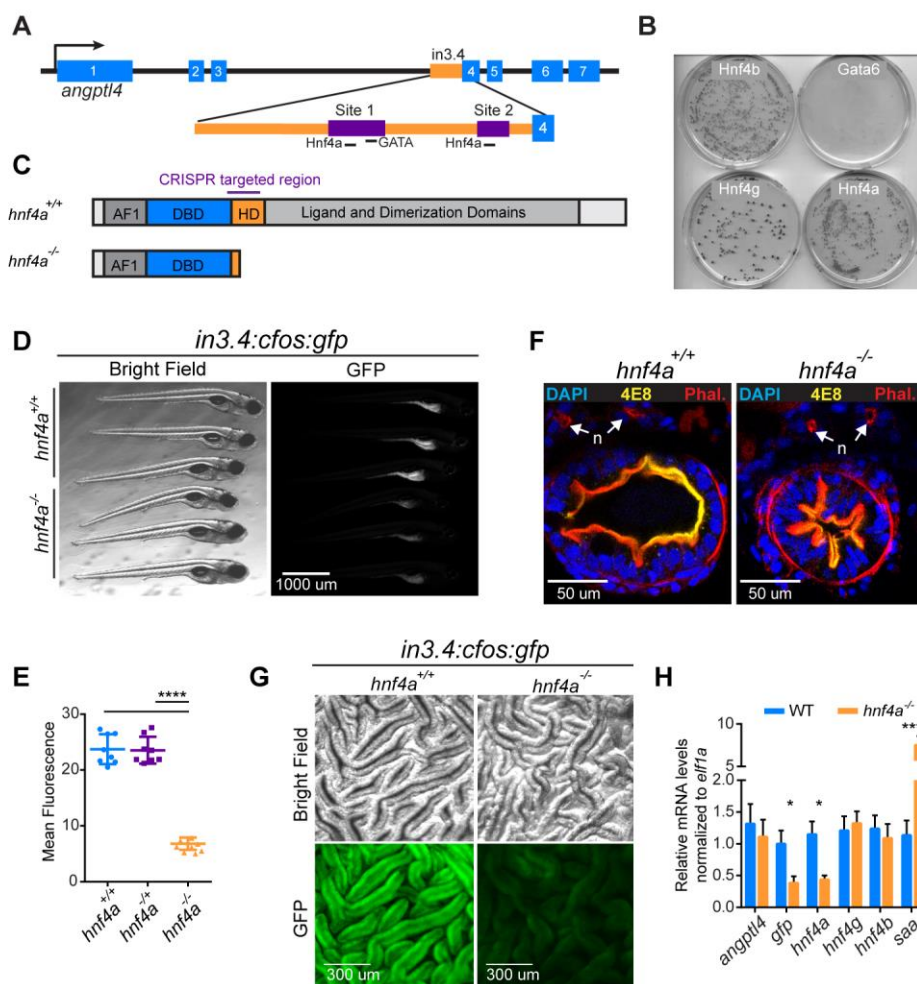
5

Figure 1

FIGURE 1. Zebrafish *hnf4a* is required for robust *in3.4:cfos:gfp* activity

(A) Schematic of the microbiota-suppressed zebrafish enhancer, in3.4, highlighting the regions required for intestinal activity (purple) which both contain putative Hnf4 binding sites (Site 1 and Site 2) (Camp et al. 2012). (B) Image of 4 plates from the Y1H assay showing the *hnf4* family of transcription factors capable of binding in3.4 and driving expression of the antibiotic resistance reporter gene. (C) Hnf4a^{+/+} and Hnf4a^{-/-} protein cartoons showing the DNA binding domain (DBD) and hinge domain (HD). We characterized the two with the largest lesions, a -41 deletion in the hinge domain and a +25 insertion in the hinge domain which both result in frame-shift early-stop codons and significantly reduced transcript. (D) Stereofluorescence GFP and bright field microscopy showing representative *hnf4a^{+/+}* (top 3) and *hnf4a^{-/-}* (bottom 3) 6dpf *in3.4:cfos:gfp* zebrafish. Genotype was blinded and samples were arranged by intensity of GFP fluorescence. (E) GFP fluorescence (mean ± sem) in *hnf4a^{+/+}* (n = 8), *hnf4a^{+/-}* (n = 8) and *hnf4a^{-/-}* (n = 8) 6dpf *in3.4:cfos:gfp* zebrafish (Two-tailed t-test: t = 17.84, 16.51, respectively, df = 14, and **** $p < 0.0001$). (F) Confocal microscopy showing representative axial cross sections in 6dpf *hnf4a^{+/+}* (n = 4) and *hnf4a[-41/-41]* (n = 4) larval zebrafish. 4e8 antibody (yellow) labels the intestinal brush border, DAPI (blue) and phalloidin (red), and nephros (n). (G) Bright field microscopy (top) and stereofluorescence GFP (bottom) for representative *hnf4a^{+/+}* (n = 3) (left) and *hnf4a^{-/-}* (n = 3) (right) dissected intestinal folds from adult *in3.4:cfos:gfp* zebrafish. (H) Relative mRNA levels (mean ± sem) in *hnf4a^{+/+}* (n = 3) and *hnf4a^{-/-}* (n = 3) adult zebrafish intestinal epithelial cell as measured by qRT-PCR. Two-tailed t-test: t = 0.93, 5.22, 6.56, 10.65, 0.75, 0.94 respectively, df = 4, and * $p < 0.05$, *** $p < 0.001$). See also Supplemental Figures S1 and S2.

102

103   of in3.4 were unknown. Using a yeast one-hybrid (Y1H) assay, we tested the capacity of 150

104   TFs expressed in the zebrafish digestive system to bind in3.4 (Supplemental Fig. S1A,B;

105   Supplemental Table S1) and detected an interaction only with *hnf4a*, *hnf4b*, and *hnf4g* (Fig. 1B).

106   When either of two predicted Hnf4 motifs in in3.4 are mutated, the Hnf4-in3.4 interaction in the

107   Y1H assay and intestinal GFP expression in *in3.4:cfos:gfp* zebrafish is strongly reduced

108   (Supplemental Fig. S1C-F). Interestingly, while *gata4*, *gata5*, and *gata6* have predicted motifs in

109   in3.4 (Camp et al. 2012) these TFs did not interact in the Y1H assay. This suggests that HNF4

110   TFs are capable of binding in3.4 directly and HNF4 binding sites are necessary for directing

111   in3.4-based transcription *in vitro* and in the intestine.

112   We hypothesized that the *hnf4* transcription factor family is required to mediate microbial

113   suppression of in3.4 activity. Although the Y1H assay demonstrated all 3 zebrafish Hnf4

114   members are capable of binding in3.4, we concentrated our efforts on understanding the

115   function of *hnf4a* because it is the most highly conserved Hnf4 family member (Supplemental

116   Fig. S1G; Supplemental Table S10) and has well-documented roles in intestinal physiology

117   (San Roman et al. 2015). To that end, we generated *hnf4a* mutant zebrafish using the

118   CRISPR/Cas9 system (Fig. 1C; Supplemental Fig. S2A-C,E). Unlike mouse whole-animal *Hnf4a*

119   knockout animals that fail to initiate visceral endoderm development and die during early

120   embryogenesis (Duncan et al. 1997), zebrafish *hnf4a* mutant animals are viable and survive to

121   sexual maturity (Supplemental Fig. S2D) providing new opportunities to study the roles of Hnf4a

122   in host-microbiota interactions.

123   To determine if *hnf4a* is essential for in3.4 activity, we crossed mutant *hnf4a* alleles into the

124   *in3.4:cfos:gfp* transgenic reporter line. GFP expression was significantly reduced in the absence

125   of *hnf4a* suggesting that *hnf4a* activates in3.4 (Fig. 1D,E,G,H). This loss of GFP expression in

126   *hnf4a*^{-/-} mutants was not associated with overt defects in brush border development or epithelial

127   polarity in larval stages (Fig. 1F), nor in the establishment of intestinal folds during adult stages

128   (Fig. 1G). However, intestinal lumen of mutant larvae was reduced in size at 6 days post

129   fertilization (dpf) compared to WT siblings (Fig. 1F; Supplemental Fig. S2F). Together, these

130   data indicate *hnf4a* is essential for robust activity of a microbiota-suppressed CRR. Unlike

131   *in3.4:cfos:gfp*, *angptl4* is expressed in multiple tissues and cell types (Camp et al. 2012). To

132   determine if intestinal *angptl4* expression is dependent on *hnf4a* function, we isolated RNA from

133   IECs from *hnf4a*^{+/+} and *hnf4*^{-/-} adult *in3.4:cfos:gfp* zebrafish and performed qRT-PCR. Adult

134   IECs (AIECs) from *hnf4a*^{-/-} have significant reductions in mRNA for *gfp*, *fabp*2 (a known Hnf4a

135   target in human cell lines) (Klapper et al. 2007), and *hnf4a* compared to *hnf4a*^{+/+} controls.

136   However, *angptl4* expression remained unchanged in *hnf4*^{-/-} AIECs compared to WT,

137   suggesting *angptl4* transcript levels in the adult intestine are regulated by additional

138   mechanisms and not solely from in3.4 or Hnf4a (Fig. 1H). Transcript levels for *hnf4g* and *hnf4b*

139   in *hnf4a*^{-/-} AIEC were also unchanged. Together, these results establish that Hnf4a is required

140   for in3.4 activity in IECs and raises the possibility that Hnf4a may have broader roles in

141   mediating host transcriptional and physiological responses to microbiota.

142   **Hnf4a activates transcription of genes that are suppressed upon microbiota colonization**

143   To better define the roles of *hnf4a* in microbiota response and other aspects of digestive

144   physiology, we used RNA-seq to compare mRNA levels from digestive tracts isolated from

145   *hnf4a*^{+/+} and *hnf4a*^{-/-} zebrafish larvae in the presence (CV) or absence of a microbiota (GF; Fig.

146   2A). Consistent with our previous studies(Rawls et al. 2004; Kanther et al. 2011), comparison of

147   wildtype zebrafish reared under CV vs GF conditions revealed differential expression of 598

148   genes that were enriched for processes such as DNA replication, oxidation reduction, and

149   response to bacterium (Fig. 2B,D; Supplemental Fig. S3D; Supplemental Tables S2, S4).

150   Strikingly, disruption of the *hnf4a* gene caused gross dysregulation of the transcriptional

151   response to microbiota colonization, with the total number of microbiota responsive genes (CV

Figure 2
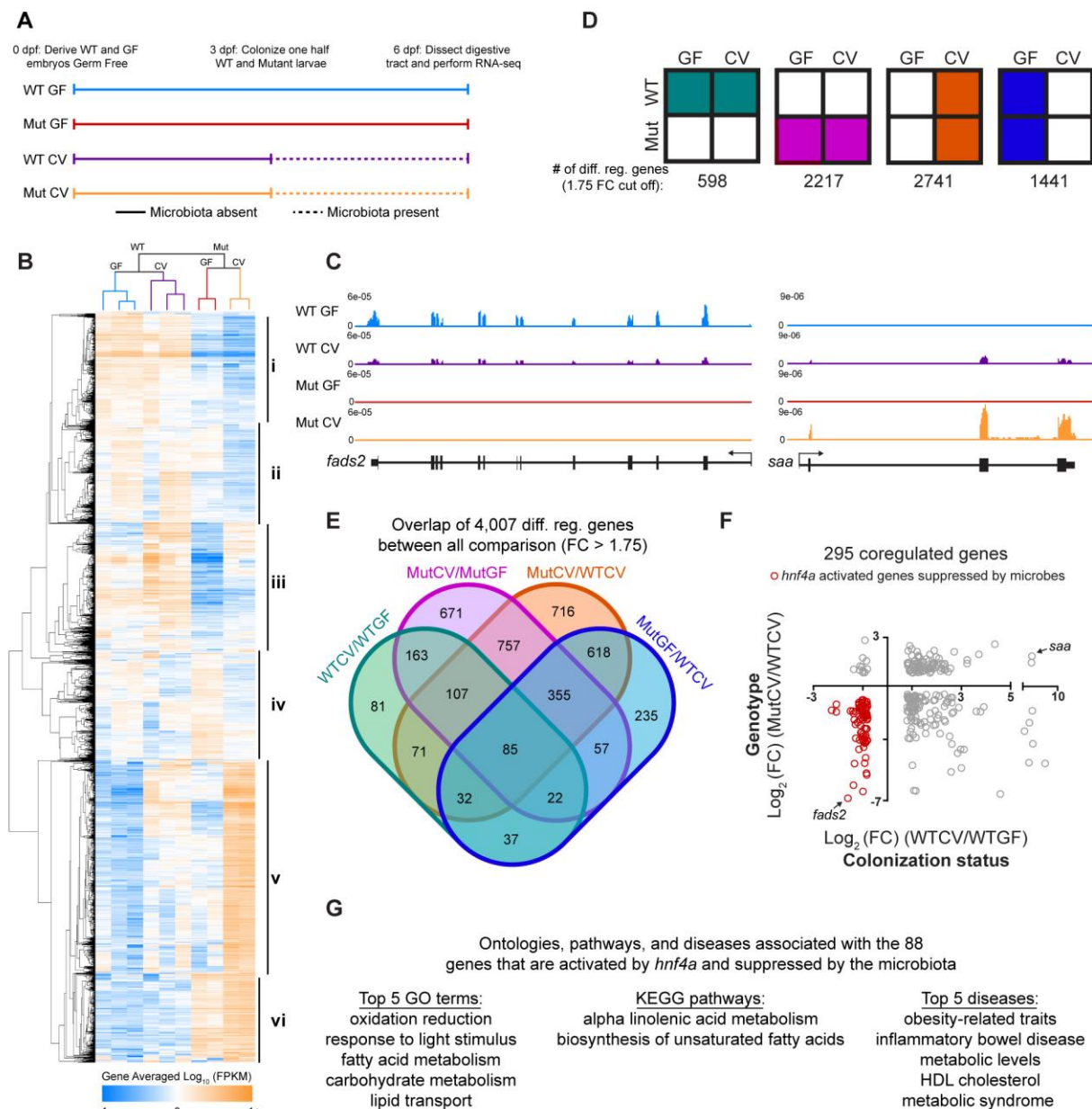
152 vs GF) increasing to 2,217. Furthermore, comparison of the *hnf4a* mutant (Mut) vs wild type

153 (WT) genotypes revealed differential expression of many genes in the CV condition (2,741

154 genes) and GF condition (1,441 genes) that inform a general role for Hnf4a in regulating genes

155 in the intestinal tract (Fig. 2D,E). Principal components analysis (Supplemental Fig. S3A) and

156 hierarchical clustering (Fig. 2B) of FPKM values indicated that *hnf4a* genotype had a complex

FIGURE 2. Hnf4a activates the majority of coregulated genes that are suppressed by the microbiota

(A) Schematic showing the experimental timeline for zebrafish digestive tract GF and CV *hnf4a*^{+/+} and *hnf4a*^{-/-} RNA-seq experiment. (B) Hierarchical relatedness tree and heatmap of differentially regulated genes in mutant and gnotobiotic zebrafish digestive tracts. Gene averaged $\log_{10}$ FPKMs for the biological replicates are represented for each of the 4,007 differentially regulated genes. (C) Representative RNA-seq signal tracks at *fatty acid-desaturase 2 (fads2)*, *serum amyloid a (saa)* loci. (D) Summary of the total number of differentially expressed genes between indicated conditions (GF and CV) and genotype (WT and *hnf4a*^{-/-} (Mut)). (E) 4-way Venn diagram showing overlaps between all 4,007 differentially regulated genes. (F) The 295 coregulated genes were plotted using the $\log_2$ (FC) calculated in the WTGF/WTCV comparison (X-axis) and WTCV/MutCV (Y-axis). The 88 out of 98 genes that are activated by *hnf4a* but suppressed by the microbiota are highlighted (red) and (G) their GO term, KEGG pathway and disease associations are listed. See also Supplemental Figure S3.

157   contribution to regulating genes involved in both response to the microbiota and digestive

158   physiology.

159   Because we found that *hnf4a* activates the microbiota-suppressed intestinal CRR, in3.4, we

160   hypothesized that this may represent a general regulatory paradigm for other microbiota-

161   influenced CRRs and genes across the genome. When we compared the 598 genes that were

162   microbiota responsive in wildtype digestive tracts with the 2,741 genes that *hnf4a* regulates in

163   CV digestive tracts we found these lists shared 295 genes that included *fads2* and *saa*, both of

164   which have human orthologs that are either implicated (*FADS1/2*) or markers (*SAA*) of IBD

165   (Plevy et al. 2013; Costea et al. 2014) (Fig. 2C-F). While loss of Hnf4a could be pleiotropic,

166   strikingly, the overlap between these subsets reveals that a disproportionate 88 of the 98

167   (~90%) microbiota-suppressed genes are activated by *hnf4a* (Fig. 2F; Supplemental Table S2).

168   These 88 genes represent almost half of all 185 genes suppressed by the microbiota. These

169   data suggest, like its role at in3.4, *hnf4a* plays a critical role in directly activating a large

170   percentage of genes that are suppressed by microbial colonization. Interestingly, despite a clear

171   enrichment of metabolism themed ontologies and pathways, we found IBD was among the top 2

172   diseases associated with genes that are activated by Hnf4a but suppressed by the microbiota

173   (Fig. 2G; Supplemental Table S11). Based on these results, we hypothesized that Hnf4a DNA

10

174   binding is lost upon microbial colonization within CRRs associated with microbiota-suppressed

175   genes.

Hnf4a binding sites are enriched in promoters near genes associated with microbiota-

regulated H3K27ac marks

178   Previous attempts to identify microbial responsive enhancers genome-wide were complicated

179   by the lack of significant changes in chromatin DNase accessibility between GF and CV IECs

180   from mouse colon and ileum (Camp et al. 2014). These previous findings suggested other

181   chromatin dynamics may be involved in regulating the IEC response to microbiota. We therefore

182   sought to provide a genomic context for understanding how the microbiota alter Hnf4a activity

183   and chromatin modifications in IECs by performing RNA-seq, DNase-seq, and ChIP-seq for the

184   enhancer histone modifications H3K4me1 and H3K27ac, and the Hnf4 TF family members

185   Hnf4g and Hnf4a in CV and GF conditions totaling 35 datasets. We conducted these

186   experiments in jejunal IEC from gnotobiotic mice because: (1) ChIP-grade antibodies for mouse

187   Hnf4a and Hnf4g are available, (2) the larger organ size provided sufficient numbers of IECs for

188   ChIP-seq experiments, and (3) we speculated that the roles of Hnf4a in host response to

189   microbiota may be conserved to mammals. We first performed DNase-seq in jejunal IEC from

190   mice reared GF or colonized for two weeks with a conventional mouse microbiota (CV) to

191   determine the impact of microbiota colonization on chromatin accessibility (Fig. 3A). In accord

192   with previous studies that that tested for chromatin accessibility in ileal or colonic IECs from GF

193   or CV mice (Camp et al. 2014), we similarly found no differential DNase hypersensitivity sites

194   (DHSs) in GF or CV jejunum (data not shown, but see Supplemental Fig. S4A; Supplemental

195   Tables S6, S8). These data indicate that gross accessibility changes in chromatin do not

196   underlie the transcription of microbiota-responsive genes in IECs.

197   To test if other metrics of chromatin utilization were dynamically regulated by microbiota, we

198   performed ChIP-seq from GF and CV mouse jejunal IECs for histone marks H3K4me1 and

199   11
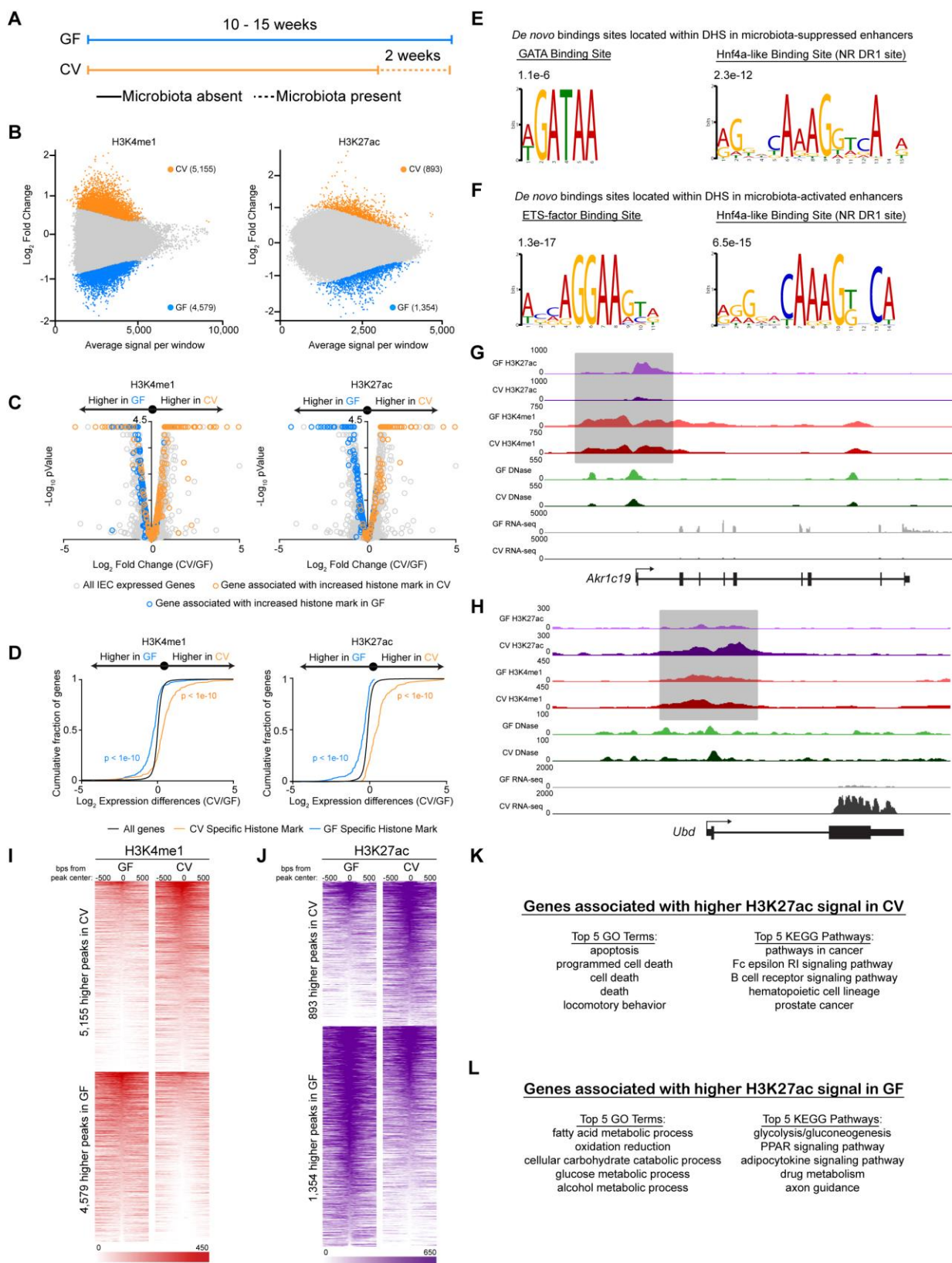
Figure 3

FIGURE 3. Microbiota selectively induce enhancer activity near genes that are upregulated upon microbiota colonization

(A) Schematic showing the gnotobiotic experimental timeline for testing mRNA levels and chromatin architecture in GF and CV. (B) MA plots from DEseq2 analysis (FDR < 0.01) of H3K4me1 (n = 3 per condition) (left) and H3K27ac (n = 2 per condition) (right) ChIP-seq from GF and CV mouse jejunal IECs. Colored dots signify regions significantly enriched for a histone mark in GF (blue) or CV (orange). We found 4,579 unique H3K4me1 and 1,354 unique H3K27ac peaks in GF and 5,155 unique H3K4me1 and 893 unique H3K27ac peaks in CV. (C) Volcano plots showing pairwise comparison of RNA expression between GF and CV jejunal IECs. Blue and orange dots represent genes associated with a region enriched for H3K4me1 (left) or H3K27ac (right) signal in GF or CV. (D) Two-sided Kolmogorov-Smirnov goodness-of-fit test shows a positive relationship on average between the presence of a region enriched for H3K4me1/H3K27ac signal in a specific colonization state and increased transcript abundance of a neighboring gene in that same colonization state. (E) Top *de novo* binding site motifs found in DHSs that are flanked by regions enriched with H3K27ac signal in GF (E) or CV (F). Representative ChIP-seq tracks highlighting a microbiota-regulated gene associated with differential histone marks in GF (G) (*Akr1c19*, *Aldo-keto reductase 1c19*) or CV (H) (*Ubd*, *Ubiquitin D*). Heatmaps showing the average GF and CV H3K4me1 (I) or H3K27ac (J) signal at the 1000 bps flanking differential sites. (K-L) GO terms and KEGG pathways enriched in genes associated with differential H3K27ac sites shown in J. See also Supplemental Figure S4.

201   H3K27ac that are enriched at poised enhancers and active enhancers, respectively (Fig. 3B).

202   By determining the single-nearest gene TSS within 10kb of the differential histone marks and

203   overlaying these data with our new RNA-seq datasets, we found that regions that gain poised

204   (H3K4me1) and activated (H3K27ac) enhancers upon colonization are associated with genes

205   that have increased transcript levels upon colonization (Fig. 3C,H-K; Supplemental Fig. S4I;

206   Supplemental Tables S3, S6, S8). Similarly, regions that lose poised and active enhancers upon

207   colonization are associated with microbiota-suppressed genes (Fig. 3C,G,I,J,L; Supplemental

208   Fig. S4J; Supplemental Tables S3, S6, S8). A two-sided Kolmogorov-Smirnov goodness-of-fit

209   test shows a positive relationship between differential H3K4me1/H3K27ac region and increased

210   transcript abundance of nearby genes in the same colonization state (Fig. 3D). Collectively, we

211   identified for the first time a genome-wide map of hundreds of newly identified microbial

212   regulated CRRs, suggesting that microbiota regulation of host genes is mechanistically linked to

213   histone modifications changes more than gross chromatin accessibility changes (Camp et al.

214   2014).

13

215   We leveraged this novel atlas of microbiota-regulated enhancers and accessible chromatin to

216   determine which TFs are predicted to bind to these regions. An unbiased analysis found that

217   Hnf4a binding site motifs were enriched in promoters of genes associated with microbiota-

218   suppressed enhancers (Supplemental Fig. S4E), and STAT1 binding site motifs were enriched

219   in promoters of genes associated with microbiota-activated enhancers (Supplemental Fig. S4F).

220   Interestingly, DHS sites associated with differentially active enhancers were enriched for two

221   different sets of TF binding sites. DHSs flanked by microbiota-inactivated enhancers were

222   enriched for nuclear receptor DR1 sites and GATA binding sites (Fig. 3E). DHS sites associated

223   with microbiota-activated enhancers were similarly enriched for the nuclear receptor DR1

224   binding sites but also for STAT/IRF-like and ETS binding sites (Fig. 3F). These data suggest

225   that nuclear receptors like Hnf4a may play a central role in IEC responses to microbial

226   colonization.

227   **Microbiota colonization is associated with a reduction in Hnf4a and Hnf4g cistrome**

228   **occupancy**

229   To directly evaluate the impact of microbiota on Hnf4a activity, we tested the plasticity of the

230   genome wide distribution of Hnf4s in response to microbial colonization. Hnf4a bound 28,901

231   and Hnf4g bound 21,875 across the genome in GF conditions in jejunal IECs with ~80% of

232   these sites being bound by both TFs. In striking contrast, the number of sites bound by Hnf4a

233   and Hnf4g in CV conditions was ~10 fold less (Fig. 4A,B; Supplemental Tables S5, S8). Of the

234   3,964 Hnf4a binding sites detected in CV there were only 267 Hnf4a sites that were specific to

235   the CV condition (Supplemental Fig. S5A,C; Supplemental Table S8). Yet, the genes associated

236   with these Hnf4a sites that are retained in CV are enriched for ontologies and pathways

237   fundamental to intestinal epithelial biology (Supplemental Fig. S5B). However, we did find that

238   the average CV Hnf4a signal was significantly increased at Hnf4a sites associated with

239   microbiota-induced genes relative to those Hnf4a sites associated with microbiota-suppressed
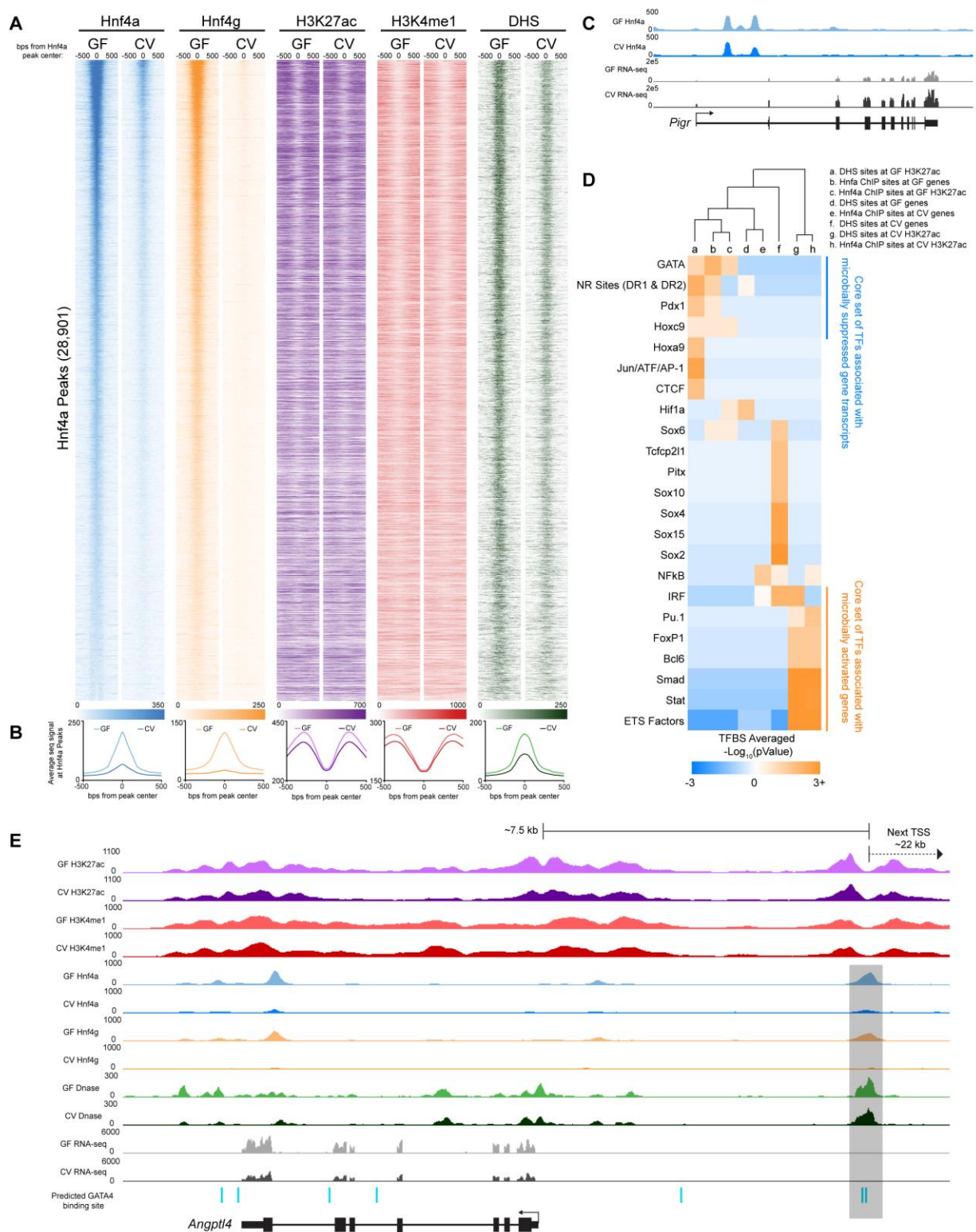
14

Figure 4

240

FIGURE 4. Microbiota colonization results in extensive loss of Hnf4a and Hnf4g DNA binding in IEC

(A) Heatmaps showing the average GF and CV ChIP-seq or DNase-seq signal at the 1000 bps flanking Hnf4a sites found in GF.(B) Line plots showing the average GF (light-colored line) and CV (dark-colored line) ChIP-seq and DNase-seq RPKM-normalized signal for the indicated TF, histone mark or DHS at the 1000 bps flanking Hnf4a sites found in GF (Hnf4a: n = 3 per condition; Hnf4g: n = 4 per condition; H3K27ac n = 2 per condition; H3K4me1: n = 3 per condition; DNase: N = 3 for CV, n = 2 for GF) . (C) Representative signal tracks highlighting a microbiota-induced gene (*Pigr*, *Polymeric immunoglobulin receptor*) that is associated with an Hnf4a peak with similar signal in both GF and CV jejunal IECs. (D) Heatmap showing the enrichment of TFBS motifs within 50 bps of the DHS or Hnf4a peak maxima. (E) Representative signal track at *Angptl4* highlighting two GATA4 sites within an Hnf4a bound region.See also Supplemental Figure S5.

241   genes, suggesting Hnf4a may play a limited role in genes upregulated by colonization

242   (Supplemental Fig. S5F). In contrast, GF Hnf4a ChIP signal was equivalent at Hnf4a sites

243   associated with microbiota-suppressed and induced genes (Supplemental Fig. S5F). We do not

244   believe that the reduction of Hnf4a binding is the result of chromatin quality in a particular

245   condition since there are genomic locations where GF and CV Hnf4a sites appeared to have

246   equivalent signal (Fig. 4C). Furthermore, ChIP enrichment in these IEC preparations for another

247   zinc finger TF, CTCF, was unaffected by microbiota colonization (Supplemental Fig. S5D). This

248   indicates that the observed reduction of Hnf4 ChIP signal in CV IECs is a result of microbiota on

249   Hnf4 binding, and is not the result of altered ChIP efficiency or sample quality in the different

250   conditions. The dramatic loss of Hnf4a and Hnf4g DNA binding upon colonization is consistent

251   with Hnf4a acting as a potent activator of microbiota-suppressed genes.

252   We further speculated that certain coregulatory sequence-specific transcription factors may also

253   contribute to regulating transcription with Hnf4 at these sites. To explore this possibility, we

254   searched for TF motifs associated with Hnf4a ChIP sites and found an enrichment of putative

255   binding sites for TFs known to be involved in small intestinal physiology (GATA and Hoxc9) as

256   well as nutrient metabolism (Pdx1) at both Hnf4a bound regions associated with genes and

257   enhancers suppressed by microbes (Fig. 4D). We similarly found GATA sites located within an

258   Hnf4a-bound CRR near murine *Angptl4* (Fig. 4E), similar to the coincident Hnf4 and GATA

259   motifs in in3.4 (Camp et al. 2012). Furthermore, binding sites for TFs known to be involved in

260   cell proliferation and cell death (ETS transcription factor family) are enriched near Hnf4a bound

261   regions that intersect microbiota-induced enhancers (Fig. 4D). Collectively our integrative

262   analyses of these novel ChIP-seq, DNase-seq, and RNA-seq datasets identifies a core set of

263   putative microbiota-responsive TFs that may interact with Hnf4a to mediate microbial control of

264   IEC gene expression. These results suggest Hnf4a plays a major role in integrating microbial

265   signals to regulate gene expression, and raise the possibility that this novel microbiota-Hnf4a

266   axis might contribute to human disease.

267   **Microbiota-mediated suppression of Hnf4a may contribute to IBD pathogenesis**

268   Both Hnf4a and the intestinal microbiota have been separately implicated in the pathogenesis of

269   inflammatory bowel diseases such as Crohn's disease (CD) and ulcerative colitis (UC) (Ahn et

270   al. 2008; Sartor and Wu 2016). However, a mechanistic link between microbiota and Hnf4a in

271   the context of IBD pathogenesis has not been established. Previous transcriptomic studies have

272   identified genes differentially expressed in ileal (iCD) and colonic CD (cCD) and UC (Arijs et al.

273   2009; Haberman et al. 2014) biopsies. We queried these human gene lists to identify one-to-

274   one orthologs in mice, and referenced them against our new gnotobiotic mouse jejunal Hnf4a

275   ChIP-seq data (Fig. 5A). Strikingly, the majority of human genes downregulated in all of these

276   IBD datasets have mouse orthologs that are associated with an Hnf4a-bound region (Fig. 5B,C;

277   Supplemental Table S7). Focusing on the iCD dataset from the largest of these previous studies

278   (Haberman et al. 2014), we found differential iCD genes associated with Hnf4a sites are

279   enriched for distinct ontologies and pathways that are dysregulated in IBD (Fig. 5H-K). In

280   contrast to IBD, analysis of a transcriptomic dataset from human necrotizing enterocolitis (NEC)

281   (Tremblay et al. 2016) revealed significantly less Hnf4a-bound regions near genes both induced

282   and suppressed in NEC (Fig. 5B,C). These data indicate microbiota-dependent and microbiota-

283   independent suppression of Hnf4a activity may play an important role in IBD pathologies, but

284   not NEC.

285   17

Figure 5

286
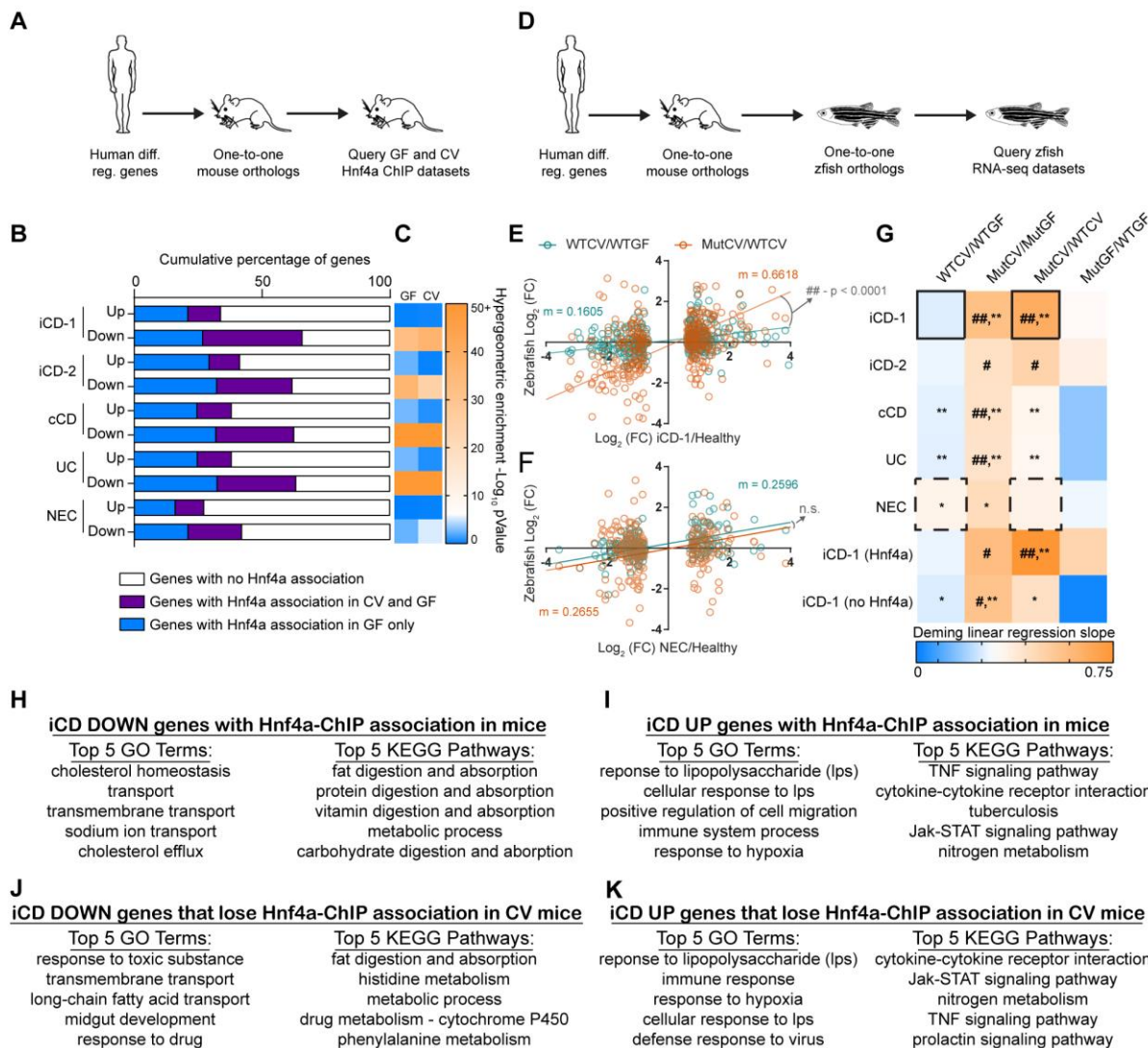
287   To assess if microbiota suppression of Hnf4a activity regulates genes differentially expressed in

288   IBD, we queried the published human IBD and NEC gene expression datasets to identify

289   human-mouse-zebrafish one-to-one-to-one orthologs that were differentially expressed in our

290   RNA-seq analysis of gnotobiotic zebrafish *hnf4a* mutants (Fig. 5D). We found ortholog

291   expression fold changes in human IBD/healthy comparisons most closely resembled the

292   expression fold changes of MutCV/MutGF and MutCV/WTCV (Fig. 5E-G). Neither the

293   WTCV/WTGF nor the MutGF/WTGF comparisons faithfully recapitulate the expression profiles

FIGURE 5. Microbiota suppression of Hnf4a activity is highly correlated with genes and intestinal processes suppressed in human IBD and conserved in zebrafish

(A) Flow chart showing the experimental design and filters used to identify IBD or NEC gene orthologs associated with mouse Hnf4a ChIP sites. (B) Bar chart showing the proportion of Hnf4a associations in GF and CV mouse jejunal IECs near human-to-mouse one-to-one gene orthologs differentially regulated in human pediatric ileal Crohn's Disease (iCD-1), adult iCD (iCD-2), adult colonic Crohn's Disease (cCD), adult ulcerative colitis (UC), or neonatal necrotizing enterocolitis (NEC). (C) Heatmap representing the $-Log_{10}$ (pValue) of the enrichment of GF or CV Hnf4a-associated genes that are differentially regulated genes in the indicated IBD datasets. pVlaues were calculated using a hypergeometric enrichment analysis and converting all Hnf4a ChIP-associated mouse genes to human orthologs (GF = 5863 genes and CV = 2119 genes). (D) Flow chart showing the experimental design and filters used to identify correlations between gnotobiotic WT or mutant zebrafish gene expression and gene orthologs differentially expressed in human IBD or NEC. Because loss of *hnf4a* function in zebrafish appeared to more closely resemble iCD signature than cCD or UC, we performed pairwise comparisons of gene orthologs that are (1) differentially regulated in human iCD and (2) have a mouse Hnf4a ChIP association. Example of Deming linear regression analysis showing the correlation of Log_2 (FC) between WTCV/WTGF (E) or MutCV/WTCV (F) zebrafish and pediatric iCD or NEC. m = slope of the line. (G) Heatmap representing slopes of Deming linear regression lines showing positive correlative relationships between the log_2 gene expression fold changes of one-to-one orthologs from human diseases compared to log_2 fold changes in zebrafish WTCV/WTGF, MutCV/MutGF, MutCV/WTCV, and MutGF/WTGF. Hash signs indicate slope of Deming linear regression lines is significantly greater than WTCV/WTGF comparison (#, $p < 0.05$; ##, $p < 0.0001$). Asterisks indicate slope of Deming linear regression line is significantly greater than MutGF/WTGF (*, $p < 0.05$; **, $p < 0.001$). Solid boxes correspond to slope of lines in panel 5D, and dashed boxes correspond to slope of lines in panel 5E. (H-K) The top 5 GO terms and the top 5 KEGG pathways for indicated gene lists.

294   of IBD/healthy comparisons. This indicates that both the microbiota and loss of *hnf4a* function

295   are necessary to induce an IBD-like gene expression profile in zebrafish. Strikingly, the positive

296   correlation and significant resemblance to the iCD-like gene signatures in the colonized *hnf4a*$^{-/-}$

297   compared to colonized *hnf4a*$^{+/+}$ zebrafish digestive tracts become even stronger when we

298   limited our analysis to one-to-one orthologs that have an association with an Hnf4a bound

299   region in mouse IECs (Fig. 5G). Together, these results suggest that Hnf4a protects the host

300   and maintains transcriptional homeostasis in the presence of a microbiota and protects against

301   an IBD-like gene expression signature.

302   **DISCUSSION**

303   Over the course of animal evolution, the intestinal epithelium has served as the primary barrier

304   between animal hosts and the complex microbial communities they harbor. IECs maintain this

305   barrier and perform their physiological roles in nutrient transport and metabolism through

306   dynamic transcriptional programs. The regulatory mechanisms that orchestrate these

307   transcriptional programs represent potential therapeutic targets for a variety of human intestinal

308   diseases including IBD. Here we discovered that Hnf4a activity and its transcriptional network

309   are suppressed by microbiota. Hnf4a is the oldest member of the nuclear receptor TF family

310   (Bridgham et al. 2010), and our findings in fish and mammals suggest that microbial

311   suppression of Hnf4a may be a conserved feature of IEC transcriptional programs present in the

312   common ancestor.

313   Our results suggest important new links between Hnf4a and microbiota in the context of human

314   IBD. IBD patients, particularly those suffering from Crohn's disease, often present with

315   decreased serum low-density lipoprotein levels and reduced total cholesterol levels compared to

316   healthy individuals (Hrabovsky et al. 2009; Agouridis et al. 2011). These serum levels are

317   consistent with reduced transcript levels for genes involved in intestinal absorption and transport

318   of lipid and cholesterol in ileal and colonic biopsies from IBD patients (Arijs et al. 2009;

319   Haberman et al. 2014). Transcription factors, including nuclear receptors like Hnf4a and Fxr, are

320   known to regulate bile acid production, lipid mobilization and cholesterol absorption have

321   already been implicated in IBD (Ahn et al. 2008; Nijmeijer et al. 2011). However, our work is the

322   first to demonstrate a role for microbiota in suppressing Hnf4a that may ultimately affect IBD

323   pathogenesis. Hnf4a has been shown to play key roles in anti-oxidative and anti-inflammatory

324   defense mechanisms (Marcil et al. 2010) so aberrant microbial suppression could promote a

325   chronic inflammatory state. Hnf4a target genes are downregulated in human IBD (Arijs et al.

326   2009; Haberman et al. 2014) and mouse experimental colitis, and the Hnf4a target ApoA1 has

327   been shown to be protective against intestinal inflammation in mice (Gkouskou et al. 2016). We

328   speculate that the genes governed by this novel microbiota-Hnf4a axis may include additional

329   anti- and pro-inflammatory factors that could provide new targets for IBD therapy.

20

330   Our results reveal similar effects of microbiota colonization and experimental colitis on Hnf4a

331   cistrome occupancy, but the underlying molecular mechanisms are unresolved. DSS induced

332   colitis results in reduced Hnf4a protein levels and altered cellular localization (Chahar et al.

333   2014), however our results indicate the microbiota neither reduce Hnf4a protein levels nor

334   impact its nuclear localization in jejunal IECs two weeks after colonization (Supplemental Fig.

335   S5H,I). Colonization of GF mice with microbiota initiates a transcriptional adaptation in the

336   intestine that progresses for several weeks before reaching homeostasis (El Aidy et al. 2012),

337   so further studies are needed to determine if Hnf4a activity is similarly altered at other stages of

338   this adaptive process. However, these data collectively suggest that microbiota suppress Hnf4a

339   activity in the jejunum through mechanisms distinct from those utilized in experimental colitis.

340   Despite the importance of Hnf4a in digestive and metabolic health (Palanker et al. 2009;

341   Frochot et al. 2012), relatively little insight into its regulation in a biological context has been

342   reported. *In vitro* and cell culture studies have identified possible suppressors and activators of

343   Hnf4a including phosphorylation by AMPK and acetylation by CBP, both of which have been

344   shown to induce Hnf4a activity (Soutoglou et al. 2000; Hong et al. 2003). Other studies have

345   shown that Hnf4a regulation is controlled by alternative promoters which generate different

346   isoforms(Huang et al. 2009). However, we did not detect differential *Hnf4a* exon usage by

347   DEXseq (Li et al. 2015) in GF and CV mouse jejunal IECs (data not shown). Another facet of

348   Hnf4a biology that has not been adequately explored is the identity of its endogenous ligand(s).

349   Although historically considered an orphan nuclear receptor, several fatty acids including linoleic

350   acid have been identified as ligands for Hnf4a (Hertz et al. 1998; Palanker et al. 2009; Yuan et

351   al. 2009). Fatty acids are an attractive class of putative regulators of Hnf4a since the microbiota

352   are known to augment FA absorption in zebrafish enterocytes (Semova et al. 2012).

353   Identification of Hnf4a ligands or other co-regulatory factors that mediate microbial control of

354   Hnf4a could provide novel therapeutic targets for IBD (Mbodji et al. 2013).

21

355 In our attempt to understand how the microbiota regulate Hnf4a activity and host gene

356 transcription, we were motivated to investigate if microbiota impact histone modification and

357 chromatin accessibility in the mouse jejunum. Our findings support the model that microbiota

358 alter IEC gene expression by affecting TF binding and histone modification at tissue-defined

359 open chromatin sites (Camp et al. 2014). We provide the genomic addresses of hundreds of

360 microbiota-regulated enhancers as well as the genes associated with these enhancers and

361 Hnf4a binding sites. Similar to other findings in intraepithelial lymphocytes (Semenkovich et al.

362 2016), our work demonstrates a clear microbial contribution to the modification of the histone

363 landscape in IECs and provides another important layer of regulation that orchestrate microbiota

364 regulation of host genes involved in intestinal physiology and human disease. We were also

365 able to establish a link between microbiota-regulated genes and enhancers and NR binding

366 sites. These NR binding sites are coincident with a core set of TFs that are enriched near

367 microbiota-suppressed enhancers/genes (GATA) or induced enhancers/genes (ETS-factors and

368 IRF) (Supplemental Fig. S6). Coregulation by other TFs represents one possible mode of Hnf4a

369 regulation by which the microbiota could suppress Hnf4a activity without impacting the gene

370 transcription of all Hnf4a-associated genes.

371 **METHODS**

372 **Yeast 1-Hybrid ORFeome Screen:**

373 The yeast 1-hybrid ORFeome screen was performed using the Clontech MatchmakerTM Gold

374 Yeast One-hybrid Library Screening System (cat. 630491) protocol with the following

375 exceptions: The Y1HGold yeast strain was transformed using standard yeast transformation

376 procedures with BstBI digested pBait-AbAi containing either the WT or a SDM in3.4 or the p53

377 binding site sequence, and positive transformants were selected on SD/-URA media. In

378 addition, a ORFeome library consisting of 148 zebrafish transcription factors cloned from adult

379   zebrafish liver (Supplemental Table S1) into pDEST22 prey vectors containing an N-terminal

380   GAL4-activation domain was utilized (Boyle et al. 2016). For additional information, see

381   Supplemental Methods.

Zebrafish Transgenesis and Imaging:

383   Co-injections of Tol2 SDM or WT in3.4:cfos:gfp plasmid and transposase mRNA were

384   performed as described (Camp et al., 2012) with the following exceptions: 50 – 100 zebrafish

385   embryos were injected at the 1–2 cell stage with approximately 69 pg of plasmid DNA at a

386   DNA:transposase ratio of 1:2. Three mosaic patches within a given tissue of an imaged fish

387   were quantified for mean fluorescence intensity and averaged. Statistical significance was

388   analyzed using Kruskal-Wallis one-way analysis of variance and Dunn's multiple comparison

389   test using GraphPad Prism software. For additional information, see Supplemental Methods.

Zebrafish Mutagenesis:

391   Targeted gene deletion of the *hnf4a* gene was performed using CRISPR/Cas9 nuclease RNA-

392   guided genome editing targeting the fourth exon of *hnf4a*. The guide RNA sequences were

393   designed using "CRISPR Design Tool" (http://crispr.mit.edu/). Guide RNAs (Supplemental

394   Table S9) were generated from BamHI (New England Biolabs R0136L) digested pT7-gRNA

395   plasmid (a gift from Wenbiao Chen and available from Addgene:

396   http://www.addgene.org/46759/) and by performing an *in vitro* transcription reaction using

397   MEGAshortscript T7 kit (Ambion/Invitrogen AM1354). For additional information, see

398   Supplemental Methods.

Mouse IEC Isolation for DNAse, ChIP and RNA-seq:

400   Mice were euthanized under CO_2 and cervical dislocation and placed on a chilled wax

401   dissection pad. The small intestine was removed from the mouse and the jejunum was excised

402   from the duodenum and ileum. Duodenum was defined as the anterior 5 cm of the midgut and

403   ileum was defined as posterior 6 cm of midgut as described (Camp, et al 2014). Adipose and

404   vasculature were removed from the tissue. The jejunum was opened longitudinally along the

405   length of the tissue, exposing the lumen and epithelial cell layer. Luminal debris was washed

406   away from the epithelia with ice cold sterile PBS. The tissue was temporarily stored in 10 ml of

407   ice cold sterile PBS with 1x Protease Inhibitor (Complete EDTA-Free, Roche 1187350001) and

408   10 uM Y-27632 (ROCK I inhibitor, Selleck Chemicals S1049) to inhibit spontaneous apoptosis.

409   The jejunum was moved into a 15 ml conical tube containing 3 mM EDTA in PBS with 1x

410   protease inhibitor and 10 uM Y-27632. The tissue was placed on a nutator in a cold room for 15

411   minutes. The jejunum was removed from the 3 mM EDTA and placed on an ice cold glass petri

412   dish with PBS containing 1mM MgCl2 and 2 mM CaCl2 with protease inhibitors and 10 uM Y-

413   27632. Villi were scraped off of the tissue using a sterile plastic micropipette and placed into a

414   new 15 ml conical tube. The isolated IECs were then crosslinked for ChIP or used for DNAse-

415   seq or RNA-seq. For additional information, see Supplemental Methods.

416   **Mouse Intestine Immunofluorescence and Western Blot:**

417   Mid-jejunal tissue was dissected and cleaned as in the IEC villi isolation above. The whole,

418   splayed open tissue was pinned to 3% agarose and fixed in 4% PFA overnight with gentle

419   agitation at 4°C. The fixed tissue was washed 4 times with PBS for 15 minutes. The tissue was

420   then permeabilized in PBS with 0.5% Tween 20 for 1.5 hours at room temperature. Following

421   permeabilization, the tissue was blocked in 5% donkey serum in PBS with 0.1% Tween 20 for 2

422   hours at room temperature, incubated in primary and secondary antibodies and imaged on a

423   Leica SP8 confocal microscope. Western blots were performed on non-crosslinked IEC lysates

424   (see below) using standard chemoluminescence Western blot protocols. The western blot

425   shown in Supplemental Fig. S5H is a representative of two experiments.   For additional

426   information, see Supplemental Methods.

24

427   **Bioinformatic and Statistical analysis:**

428   Sample sizes for zebrafish experiments (noted in figure legends) were selected based on

429   genotype availability and transgenesis efficiency. All sample collection was performed two or

430   more times on independent days. For sequencing experiments, statistical calls for differential

431   gene expression were made by Cuffdiff using parameters stated above. For the zebrafish RNA-

432   seq experiment Next-Gen sequencing was performed once and at the same time to avoid batch

433   effects: WTGF and WTCV (n = 3); MutGF and MutCV (n = 2). We originally collected n = 3

434   MutGF and MutCV biological replicates, however, using pre-established criteria and to avoid

435   RNA contamination, we excluded one biological replicate from all analysis from these groups

436   because of sequencing reads that mapped within the deleted *hnf4a* exon in the *hnf4a*^{-/-}

437   genotype.

438   GF mice were randomly chosen by gnotobiotic staff for microbiota colonization (CV) based on

439   their availability and litter sizes. All sample collection was performed two or more times per

440   condition on independent days. GF and CV mouse samples were collected on different days.

441   For sequencing experiments, statistical calls for differential gene expression and differential

442   peak calls were made by Cuffdiff, MACS2, and DEseq2 using parameters stated above. For the

443   mouse RNA-seq experiment Next-Gen sequencing was performed once and at the same time

444   to avoid batch effects: GF (n = 2) and CV (n = 2). Paired GF and CV ChIP and library

445   amplification was performed simultaneously. Typically, biological ChIP replicates were

446   sequenced on different days and were always paired with the other condition (i.e. CV and GF

447   were always sequenced together). The number of biological ChIP replicates (noted in figure

448   legends) was dependent on reproducibility between ChIP samples and/or our ability to

449   determine statistical differential sites using DEseq2 (for H3K4me1 and H3K27ac).

450   All statistical metrics (except where otherwise noted) were performed in Graphpad Prism 7.01.

451   Deming linear regression was used for Fig. 5 because it is a stronger and more accurate

452   assessment of correlation when both the x and y variables have experimental error. Details

453   regarding the other statistical tests used in this study can be found in the figure legends or

454   above.

455   For additional information, see Supplemental Methods.

456   **Dataset Accessions:**

457   Sequence datasets are available at GEO accession number GSE90462.

458   **ACKNOWLEDGEMENTS**

465

REFERENCES

466

467 Agouridis AP, Elisaf M, Milionis HJ. 2011. An overview of lipid abnormalities in patients with
468 inflammatory bowel disease. *Ann Gastroenterol* **24**: 181-187.

469 Ahn SH, Shah YM, Inoue J, Morimura K, Kim I, Yim S, Lambert G, Kurotani R, Nagashima K,
470 Gonzalez FJ et al. 2008. Hepatocyte nuclear factor 4alpha in the intestinal epithelial cells
471 protects against inflammatory bowel disease. *Inflamm Bowel Dis* **14**: 908-920.

472 Alenghat T, Osborne LC, Saenz SA, Kobuley D, Ziegler CG, Mullican SE, Choi I, Grunberg S,
473 Sinha R, Wynosky-Dolfi M et al. 2013. Histone deacetylase 3 coordinates commensal-bacteria-
474 dependent intestinal homeostasis. *Nature* **504**: 153-157.

475 Arijs I, De Hertogh G, Lemaire K, Quintens R, Van Lommel L, Van Steen K, Leemans P,
476 Cleynen I, Van Assche G, Vermeire S et al. 2009. Mucosal gene expression of antimicrobial
477 peptides in inflammatory bowel disease before and after first infliximab treatment. *PLoS One* **4**:
478 e7984.

479 Bäckhed F, Ding H, Wang T, Hooper LV, Koh GY, Nagy A, Semenkovich CF, Gordon JI. 2004.
480 The gut microbiota as an environmental factor that regulates fat storage. *Proc Natl Acad Sci U S*
481 *A* **101**: 15718-15723.

482 Bates JM, Akerlund J, Mittge E, Guillemin K. 2007. Intestinal alkaline phosphatase detoxifies
483 lipopolysaccharide and prevents inflammation in zebrafish in response to the gut microbiota.
484 *Cell Host Microbe* **2**: 371-382.

485 Berndt SI Gustafsson S Magi R Ganna A Wheeler E Feitosa MF Justice AE Monda KL Croteau-
486 Chonka DC Day FR et al. 2013. Genome-wide meta-analysis identifies 11 new loci for
487 anthropometric traits and provides insights into genetic architecture. *Nat Genet* **45**: 501-512.

488 Boyle G, Richter K, Priest HD, Traver D, Mockler TC, Chang JT, Kay SA, Breton G. 2016.
489 Comparative analysis of vertebrate diurnal/circadian transcriptomes. *PloS One* **In Press**.

490 Bridgham JT, Eick GN, Larroux C, Deshpande K, Harms MJ, Gauthier ME, Ortlund EA, Degnan
491 BM, Thornton JW. 2010. Protein evolution by molecular tinkering: diversification of the nuclear
492 receptor superfamily from a ligand-dependent ancestor. *PLoS Biol* **8**.

493 Camp JG, Frank CL, Lickwar CR, Guturu H, Rube T, Wenger AM, Chen J, Bejerano G,
494 Crawford GE, Rawls JF. 2014. Microbiota modulate transcription in the intestinal epithelium
495 without remodeling the accessible chromatin landscape. *Genome Res* **24**: 1504-1516.

496 Camp JG, Jazwa AL, Trent CM, Rawls JF. 2012. Intronic cis-regulatory modules mediate tissue-
497 specific and microbial control of angptl4/fiaf transcription. *PLoS Genet* **8**: e1002585.

498 Chahar S, Gandhi V, Yu S, Desai K, Cowper-Sal-lari R, Kim Y, Perekatt AO, Kumar N,
499 Thackray JK, Musolf A et al. 2014. Chromatin profiling reveals regulatory network shifts and a
500 protective role for hepatocyte nuclear factor 4alpha during colitis. *Mol Cell Biol* **34**: 3291-3304.

501 Chellappa K, Deol P, Evans JR, Vuong LM, Chen G, Briancon N, Bolotin E, Lytle C, Nair MG,
502 Sladek FM. 2016. Opposing roles of nuclear receptor HNF4alpha isoforms in colitis and colitis-
503 associated colon cancer. *Elife* **5**.

504 Costea I, Mack DR, Lemaitre RN, Israel D, Marcil V, Ahmad A, Amre DK. 2014. Interactions
505 between the dietary polyunsaturated fatty acid ratio and genetic factors determine susceptibility
506 to pediatric Crohn's disease. *Gastroenterology* **146**: 929-931.

507 Creyghton MP, Cheng AW, Welstead GG, Kooistra T, Carey BW, Steine EJ, Hanna J, Lodato
508 MA, Frampton GM, Sharp PA et al. 2010. Histone H3K27ac separates active from poised
509 enhancers and predicts developmental state. *Proc Natl Acad Sci U S A* **107**: 21931-21936.

510 Darsigny M, Babeu JP, Dupuis AA, Furth EE, Seidman EG, Levy E, Verdu EF, Gendron FP,
511 Boudreau F. 2009. Loss of hepatocyte-nuclear-factor-4alpha affects colonic ion transport and
512 causes chronic inflammation resembling inflammatory bowel disease in mice. *PLoS One* **4**:
513 e7609.

514 Duncan SA, Nagy A, Chan W. 1997. Murine gastrulation requires HNF-4 regulated gene
515 expression in the visceral endoderm: tetraploid rescue of Hnf-4(-/-) embryos. *Development* **124**:
516 279-287.

517 El Aidy S, van Baarlen P, Derrien M, Lindenbergh-Kortleve DJ, Hooiveld G, Levenez F, Dore J,
518 Dekker J, Samsom JN, Nieuwenhuis EE et al. 2012. Temporal and spatial interplay of
519 microbiota and intestinal mucosa drive establishment of immune homeostasis in
520 conventionalized mice. *Mucosal Immunol* **5**: 567-579.

521 Evans RM, Mangelsdorf DJ. 2014. Nuclear Receptors, RXR, and the Big Bang. *Cell* **157**: 255-
522 266.

523 Franke A, Hampe J, Rosenstiel P, Becker C, Wagner F, Hasler R, Little RD, Huse K, Ruether A,
524 Balschun T et al. 2007. Systematic association mapping identifies NELL1 as a novel IBD
525 disease gene. *PLoS One* **2**: e691.

526 Frochot V, Alqub M, Cattin AL, Carriere V, Houllier A, Baraille F, Barbot L, Saint-Just S, Ribeiro
527 A, Lacasa M et al. 2012. The transcription factor HNF-4alpha: a key factor of the intestinal
528 uptake of fatty acids in mouse. *Am J Physiol Gastrointest Liver Physiol* **302**: G1253-1263.

529 Gkouskou KK, Ioannou M, Pavlopoulos GA, Georgila K, Siganou A, Nikolaidis G, Kanellis DC,
530 Moore S, Papadakis KA, Kardassis D et al. 2016. Apolipoprotein A-I inhibits experimental colitis
531 and colitis-propelled carcinogenesis. *Oncogene* **35**: 2496-2505.

532 Haberman Y, Tickle TL, Dexheimer PJ, Kim MO, Tang D, Karns R, Baldassano RN, Noe JD,
533 Rosh J, Markowitz J et al. 2014. Pediatric Crohn disease patients exhibit specific ileal
534 transcriptome and microbiome signature. *J Clin Invest* **124**: 3617-3633.

535 Hertz R, Magenheim J, Berman I, Bar-Tana J. 1998. Fatty acyl-CoA thioesters are ligands of
536 hepatic nuclear factor-4alpha. *Nature* **392**: 512-516.

537 Hong YH, Varanasi US, Yang W, Leff T. 2003. AMP-activated protein kinase regulates
538 HNF4alpha transcriptional activity by inhibiting dimer formation and decreasing protein stability.
539 *J Biol Chem* **278**: 27495-27501.

540 Hrabovsky V, Zadak Z, Blaha V, Hyspler R, Karlik T, Martinek A, Mendlova A. 2009. Cholesterol
541 metabolism in active Crohn's disease. *Wien Klin Wochenschr* **121**: 270-275.

542 Huang J, Levitsky LL, Rhoads DB. 2009. Novel P2 promoter-derived HNF4alpha isoforms with
543 different N-terminus generated by alternate exon insertion. *Exp Cell Res* **315**: 1200-1211.

544 Kamada N, Seo SU, Chen GY, Nunez G. 2013. Role of the gut microbiota in immunity and
545 inflammatory disease. *Nat Rev Immunol* **13**: 321-335.

546 Kanther M, Sun X, Muhlbauer M, Mackey LC, Flynn EJ, 3rd, Bagnat M, Jobin C, Rawls JF.
547 2011. Microbial colonization induces dynamic temporal and spatial patterns of NF-kappaB
548 activation in the zebrafish digestive tract. *Gastroenterology* **141**: 197-207.

549 Klapper M, Bohme M, Nitz I, Doring F. 2007. The human intestinal fatty acid binding protein
550 (hFABP2) gene is regulated by HNF-4alpha. *Biochem Biophys Res Commun* **356**: 147-152.

551 Krautkramer KA, Kreznar JH, Romano KA, Vivas EI, Barrett-Wilt GA, Rabaglia ME, Keller MP,
552 Attie AD, Rey FE, Denu JM. 2016. Diet-Microbiota Interactions Mediate Global Epigenetic
553 Programming in Multiple Host Tissues. *Mol Cell* **64**: 982-992.

554 Li Y, Rao X, Mattox WW, Amos CI, Liu B. 2015. RNA-Seq Analysis of Differential Splice
555 Junction Usage and Intron Retentions by DEXSeq. *PLoS One* **10**: e0136653.

556 Marcil V, Seidman E, Sinnett D, Boudreau F, Gendron FP, Beaulieu JF, Menard D, Precourt LP,
557 Amre D, Levy E. 2010. Modification in oxidative stress, inflammation, and lipoprotein assembly
558 in response to hepatocyte nuclear factor 4alpha knockdown in intestinal epithelial cells. *J Biol*
559 *Chem* **285**: 40448-40460.

560 Marcil V, Sinnett D, Seidman E, Boudreau F, Gendron FP, Beaulieu JF, Menard D, Lambert M,
561 Bitton A, Sanchez R et al. 2012. Association between genetic variants in the HNF4A gene and
562 childhood-onset Crohn's disease. *Genes Immun* **13**: 556-565.

563 Marjoram L, Alvers A, Deerhake ME, Bagwell J, Mankiewicz J, Cocchiaro JL, Beerman RW,
564 Willer J, Sumigray KD, Katsanis N et al. 2015. Epigenetic control of intestinal barrier function
565 and inflammation in zebrafish. *Proc Natl Acad Sci U S A* **112**: 2770-2775.

566 Mbodji K, Charpentier C, Guerin C, Querec C, Bole-Feysot C, Aziz M, Savoye G, Dechelotte P,
567 Marion-Letellier R. 2013. Adjunct therapy of n-3 fatty acids to 5-ASA ameliorates inflammatory
568 score and decreases NF-kappaB in rats with TNBS-induced colitis. *J Nutr Biochem* **24**: 700-705.

569 Meddens CA, Harakalova M, van den Dungen NA, Foroughi Asl H, Hijma HJ, Cuppen EP,
570 Bjorkegren JL, Asselbergs FW, Nieuwenhuis EE, Mokry M. 2016. Systematic analysis of
571 chromatin interactions at disease associated loci links novel candidate genes to inflammatory
572 bowel disease. *Genome Biol* **17**: 247.

573 Morgun A, Dzutsev A, Dong X, Greer RL, Sexton DJ, Ravel J, Schuster M, Hsiao W, Matzinger
574 P, Shulzhenko N. 2015. Uncovering effects of antibiotics on the host and microbiota using
575 transkingdom gene networks. *Gut* **64**: 1732-1743.

576 Nijmeijer RM, Gadaleta RM, van Mil SW, van Bodegraven AA, Crusius JB, Dijkstra G, Hommes
577 DW, de Jong DJ, Stokkers PC, Verspaget HW et al. 2011. Farnesoid X receptor (FXR)
578 activation and FXR genetic variation in inflammatory bowel disease. *PLoS One* **6**: e23745.

579   Palanker L, Tennessen JM, Lam G, Thummel CS. 2009. Drosophila HNF4 regulates lipid
580   mobilization and beta-oxidation. *Cell Metab* **9**: 228-239.

581   Plevy S, Silverberg MS, Lockton S, Stockfisch T, Croner L, Stachelski J, Brown M, Triggs C,
582   Chuang E, Princen F et al. 2013. Combined serological, genetic, and inflammatory markers
583   differentiate non-IBD, Crohn's disease, and ulcerative colitis patients. *Inflamm Bowel Dis* **19**:
584   1139-1148.

585   Rawls JF, Samuel BS, Gordon JI. 2004. Gnotobiotic zebrafish reveal evolutionarily conserved
586   responses to the gut microbiota. *Proc Natl Acad Sci U S A* **101**: 4596-4601.

587   San Roman AK, Aronson BE, Krasinski SD, Shivdasani RA, Verzi MP. 2015. Transcription
588   factors GATA4 and HNF4A control distinct aspects of intestinal homeostasis in conjunction with
589   transcription factor CDX2. *J Biol Chem* **290**: 1850-1860.

590   Sartor RB, Wu GD. 2016. Roles for Intestinal Bacteria, Viruses, and Fungi in Pathogenesis of
591   Inflammatory Bowel Diseases and Therapeutic Approaches. *Gastroenterology*
592   doi:10.1053/j.gastro.2016.10.012.

593   Semenkovich NP, Planer JD, Ahern PP, Griffin NW, Lin CY, Gordon JI. 2016. Impact of the gut
594   microbiota on enhancer accessibility in gut intraepithelial lymphocytes. *Proc Natl Acad Sci U S*
595   *A* doi:10.1073/pnas.1617793113.

596   Semova I, Carten JD, Stombaugh J, Mackey LC, Knight R, Farber SA, Rawls JF. 2012.
597   Microbiota regulate intestinal absorption and metabolism of fatty acids in the zebrafish. *Cell*
598   *Host Microbe* **12**: 277-288.

599   Soutoglou E, Katrakili N, Talianidis I. 2000. Acetylation regulates transcription factor activity at
600   multiple levels. *Mol Cell* **5**: 745-751.

601   Stegmann A, Hansen M, Wang Y, Larsen JB, Lund LR, Ritie L, Nicholson JK, Quistorff B,
602   Simon-Assmann P, Troelsen JT et al. 2006. Metabolome, transcriptome, and bioinformatic cis-
603   element analyses point to HNF-4 as a central regulator of gene expression during enterocyte
604   differentiation. *Physiol Genomics* **27**: 141-155.

605   Thaiss Christoph A, Levy M, Korem T, Dohnalová L, Shapiro H, Jaitin Diego A, David E, Winter
606   Deborah R, Gury-BenAri M, Tatirovsky E et al. 2016. Microbiota Diurnal Rhythmicity Programs
607   Host Transcriptome Oscillations. *Cell* **167**: 1495-1510.e1412.

608   Tremblay E, Thibault MP, Ferretti E, Babakissa C, Bertelle V, Bettolli M, Burghardt KM,
609   Colombani JF, Grynspan D, Levy E et al. 2016. Gene expression profiling in necrotizing
610   enterocolitis reveals pathways common to those reported in Crohn's disease. *BMC Med*
611   *Genomics* **9**: 6.

612   Yuan X, Ta TC, Lin M, Evans JR, Dong Y, Bolotin E, Sherman MA, Forman BM, Sladek FM.
613   2009. Identification of an endogenous ligand bound to a native orphan nuclear receptor. *PLoS*
614   *One* **4**: e5609.

615